orientation. Preliminary examination and data collection were performed on a Syntex $P2_1$ diffractometer as described in Table I. Two check reflections were measured after every 98 data reflections; the intensities of these standards remained constant within experimental error throughout data collection. From the systematic absences of $h0l$ ($l = 2n$) and $0k0$ ($k = 2n$) and from the subsequent least-squares refinement, the space group was determined to be $P2_1/c$ [No. 14]. A total of 6210 reflections were collected in the $+h,+k,\pm l$ octants (5541 unique) in the range $2° \leq 2\theta \leq 50°$, with 3355 reflections having $I \geq 3\sigma(I)$. Lorentz and polarization corrections were applied to the data, and an empirical absorption correction was made.[48] The agreement factors for the 561 observed and accepted reflections were 3.2% on the basis of I and 2.3% on the basis of F_o. The structure was solved by using the Patterson heavy-atom method and difference Fourier syntheses and refined in full-matrix least squares. Hydrogen atoms were placed in calculated positions (C-H = 0.95 Å), constrained to ride on the atom to which they were bonded, and included in the refinement. The largest peak in the final difference Fourier map was 1.13 (10) e/Å^3. All calculations were performed on a VAX computer using SDP/VAX.[49]

Hydrolysis of (PhC≡CPh)Ta(NAr)Cl(py)$_2$ (13) and (C(CMe$_3$)=CHCH=C(CMe$_3$))Ta(NAr)Cl(py)$_2$ (15). A 0.054-g amount of (PhC≡CPh)Ta(NAr)Cl(py)$_2$ (**13**) was dissolved in 10 mL of Et_2O, and an excess of water (0.5 mL of 1:9 v/v H_2O/acetone) was added dropwise at room temperature. This mixture was stirred for 20 min, over which time the yellow solution decolorized and a white precipitate formed. The solvent was removed from this mixture, and the hydrolysis products were extracted with 10 mL of Et_2O and filtered through Celite. The solvent was removed in vacuo to provide a white oily solid. Only *cis*-PhCH=CHPh (and no free PhC≡CPh) was observed in the hydrolysis products by ^{1}H NMR (C_6D_6). Compound **15**, (C(CMe$_3$)=CHCH=C(CMe$_3$))Ta(NAr)Cl(py)$_2$, was hydrolyzed, and the hydrolysis product was identified as (*E*,*E*)-Me$_3$CCH=CHCH=CHCMe$_3$, by a workup procedure analogous to that described above for compound **13**. These hydrolysis reactions also produce H_2NAr in high yield (^{1}H NMR spectroscopy).

Acknowledgment is made to the donors of the Petroleum Research Fund, administered by the American Chemical Society, for support of this research. We also acknowledge support from the U.S. Army Research Office (Short Term Innovative Research Program). We thank Drs. Ian M. Gardiner and Roy L. Johnston for helpful discussions and Pamela S. Nicholls for experimental assistance in the early stages of this research.

Supplementary Material Available: Full details of the structure solution, tables of atomic positional and thermal parameters for Ta(N-2,6-C_6H_3-*i*-Pr$_2$)(O-2,6-C_6H_3Me$_2$)Cl$_2$(C_5H_5N)$_2$, full tables of bond distances and angles, and tables of least-squares planes and dihedral angles (15 pages); listings of observed and calculated structure factor amplitudes (32 pages). Ordering information is given on any current masthead page.

(48) Walker, N.; Stuart, D. *Acta Crystallogr.* **1983**, *A39*, 158.
(49) Frenz, B. A. In *Computing in Crystallography*; Schenk, H., Olthof-Hazelkamp, R., van Konigsveld, H., Bassi, G. C., Eds.; Delft University Press: Delft, Holland, 1978; pp 64-71.

Contribution from the Zettlemoyer Center for Surface Studies and Department of Chemistry, Sinclair Laboratory No. 7, Lehigh University, Bethlehem, Pennsylvania 18015

Methanol Synthesis Catalysts Based on Cs/Cu/ZnO/M_2O_3 (M = Al, Cr, Ga): Genesis from Coprecipitated Hydrotalcite-like Precursors, Solid-State Chemistry, Morphology, and Stability

John G. Nunan,[†] Paul B. Himelfarb,[‡] Richard G. Herman,* Kamil Klier, Charles E. Bogdan,[§] and Gary W. Simmons

Received March 15, 1989

The formation, decomposition, and reconstitution of hydrotalcite-like hydroxy carbonates $(Cu_{0.4}Zn_{0.6})_6M_2(OH)_{16}CO_3{\cdot}4H_2O$ (M = Al, Cr, Ga) have been studied to determine the causes of the high long-lasting catalytic activity (M = Cr) and the severe deactivation (M = Al, Ga) of the Cu/ZnO/M_2O_3 methanol synthesis catalysts doped with cesium after thermal decomposition of the hydrotalcite-like precursors. The alumina-based (M = Al) and gallia-based (M = Ga), but not the chromia-based (M = Cr), CuO/ZnO/M_2O_3 mixed oxides that were produced by thermal treatment at 623 K of the hydrotalcite-like compounds reconstituted the original hydrotalcite-type compounds during the aqueous doping procedure carried out with the cesium formate promoter, CsOOCH. The re-formation of the Al- and Ga-containing catalysts to their hydrotalcite-like precursors is due to incomplete decomposition of the hydroxy carbonates prior to doping. Electron diffraction and transmission electron microscopy give evidence for the reconstitution reactions. The alkali-metal-promoted methanol synthesis catalyst of choice from hydrotalcite-type precursors is based on chromia.

Introduction

The most active and selective low-temperature (<573 K) low-pressure (<10 kPa) methanol synthesis catalysts are based on an intimate mixture of Cu/ZnO prepared by calcination of the coprecipitated precursors.[1,2] With these binary catalysts, it was found that the composition that gives the highest activity for methanol synthesis[3] and for methanol decomposition[4] corresponded to Cu/Zn = 30/70 mol %. It was subsequently shown that preparation of this optimized catalyst by the usual method of carbonate coprecipitation resulted in the formation of a single-phase aurichalcite precursor, $(Cu_{0.3}Zn_{0.7})_5(OH)_6(CO_3)_2$.[5] Calcination and reduction of this hydroxy carbonate resulted in a dispersed Cu/ZnO catalyst, where a significant fraction of the

[†] Present address: Allied Signal, P.O. Box 5016, Des Plaines, IL 60017.
[‡] Present address: Shell Development Co., P.O. Box 1380, Houston, TX 77001.
[§] Present address: J. T. Baker, Inc., 222 Red School Lane, Phillipsburg, NJ 08865.

(1) (a) Natta, G. In *Catalysis*; Emmett, P. H., Ed.; Reinhold: New York, 1955; Vol. 3, Chapter 8. (b) Frolich, P. K.; Fenske, M. R.; Quiggle, D. *Ind. Eng. Chem.* **1928**, *20*, 694. (c) Kostelitz, O.; Huttig, G. F. *Kolloid-Z.* **1934**, *67*, 265. (d) Collins, B. M. German Patent 2,302,658 (to Imperial Chemical Industries, Ltd.), Aug 2, 1973. (e) Davies, P.; Snowdon, F. F. U.S. Patent 3,326,956 (to Imperial Chemical Industries, Ltd.), June 20, 1967. (f) Stiles, A. B. U.S. Patent 4,111,847 (to E. I. Du Pont de Nemours and Co.), Sept 5, 1978.
(2) Klier, K. *Adv. Catal.* **1982**, *31*, 243.
(3) Herman, R. G.; Klier, K.; Simmons, G. W.; Finn, B. P.; Bulko, J. B.; Kobylinski, T. P. *J. Catal.* **1979**, *56*, 407.
(4) Frolich, P. K.; Fenske, M. R.; Taylor, P. S.; Southwich, C. A., Jr. *Ind. Eng. Chem.* **1928**, *20*, 1327.
(5) Himelfarb, P. B.; Simmons, G. W.; Klier, K.; Herman, R. G. *J. Catal.* **1985**, *93*, 442.

0020-1669/89/1328-3868$01.50/0

copper particles exhibited an epitaxial relationship with the ZnO substrate such that the Cu (211) plane was parallel to ZnO ($10\bar{1}0$) and the Cu[111] axis was parallel to the ZnO [0001] axis.[6] Other forms of copper were also suggested by optical[7] and STEM[6] analyses.

To achieve high methanol productivity and to stabilize the catalyst against deactivation, the H_2/CO reactant mixture contains carbon dioxide, e.g. $H_2/CO/CO_2 = 70/24/6$ or $80/10/10$ vol %. However, it has been shown that surface doping of the Cu/ZnO catalyst with heavy alkali metal, particularly in the form of cesium hydroxides or formates, provides a stable catalyst in CO_2-free $H_2/CO = 2.33$ synthesis gas, and indeed the productivity of the catalyst is greatly enhanced when an optimum amount of alkali metal is utilized, e.g. Cs/Cu/ZnO = 0.4/30/70 mol %.[8] Reducing the reactant H_2/CO ratio to <1.0 significantly changed the selectivity from >98% methanol toward the synthesis of higher alcohols, especially of 1-propanol and 2-methyl-1-propanol.[9,10] Under these higher alcohol synthesis conditions, a ^{13}C NMR study of the C_2–C_4 products formed over the Cu/ZnO and 0.4 mol % Cs/Cu/ZnO catalysts was performed to probe the mechanisms by which the C–C bond formation process occurred. Surprisingly, it was found that the basic cesium dopant induced a unique mechanistic pathway to the higher alcohols, i.e.

$$^{12}CH_3{}^{13}CH_2OH + {}^{12}CO/H_2 \rightarrow {}^{13}CH_3{}^{12}CH_2{}^{12}CH_2OH$$

This pathway was termed *aldol coupling with oxygen retention reversal*.[10,11]

In studying the catalytic usefulness of synthetic hydrotalcite, $Mg_6Al_2(OH)_{16}(CO_3)\cdot 4H_2O$, Reichle observed that aldol reactions readily occurred over the thermally activated (723 K) material.[12] Catalysts derived from hydrotalcite-type precursors, where Mg was replaced by Cu and Zn, have been shown to be active methanol synthesis catalysts.[13-15] A key question addressed in the present research was whether Al_2O_3-, Cr_2O_3-, and Ga_2O_3-based Cu/ZnO catalysts produced via hydrotalcite-type precursors could be successfully promoted by cesium to shift the selectivity from methanol to higher alcohols in the same way that the binary unsupported Cu/ZnO catalysts were. It was found that cesium doping of the Cu/ZnO/M_2O_3 (M = Al, Cr, Ga) catalysts inhibited the synthesis of the dimethyl ether side product (by neutralizing residual acidity of the M_2O_3 supports) and significantly enhanced the alcohol synthesis rate.[16] However, with respect to the unsupported Cs/Cu/ZnO catalyst, the product selectivity of the Cs/Cu/ZnO/Al_2O_3 catalyst was shifted toward methanol, while the Cs/Cu/ZnO/Cr_2O_3 catalyst maintained a high selectivity toward C_2^+ alcohols. To determine the cause of this difference in catalytic behavior, a detailed examination of the physicochemical properties of the catalysts was carried out, and it was found that the presence or absence of cesium promotion of higher alcohol synthesis could be correlated to specific structural changes occurring during the preparation and activation of the catalysts.

Experimental Section

Catalyst Preparation and Activation. Preparation of the hydrotalcite-like precursor involved the systematic variation of a number of variables in the coprecipitation process. These included pH, temperature, presence or absence of sodium acetate in the reaction mixture, and aging time. The chemical composition of the salt solution was kept within certain limits because the hydrotalcite structure, when Cu/Zn/Al reactants were used, had been reported[17] to occur in the compositional range of Cu/Zn < 1 and (Cu + Zn)/Al ≈ 3. In the present research, the molar ratio of the metal ions was Cu/Zn/M = 30/45/25.

The apparatus used in the preparation of the ternary precursors was designed for coprecipitation of the hydroxy carbonates at constant pH and consisted of a 3-L reaction vessel, initially containing 1 L of 1.0 M sodium acetate or distilled water, in a constant-temperature water bath, two high-precision liquid pumps that delivered the 1.0 M (Cu + Zn + M) nitrate solution (at 2.82 mL/min) and the 1.0 M Na_2CO_3 solution separately to the reaction vessel, a digital pH meter accurate to ±0.01 pH unit that controlled the rate of addition of the Na_2CO_3 solution, and a mechanical stirrer with a stirring rate of ≈200 revolutions/min. After initial adjustment of the pH of the sodium acetate solution, e.g. by Na_2CO_3 to achieve pH = 9.0 or 9.5, the reactant solutions, maintained at the designated preparation temperature, were added over a time period of 120 min and the resultant precipitate was digested for an additional 5–30 min. The reaction vessel was then removed from the water bath, the precipitate was allowed to settle for 20 min, and the supernatant was decanted. After addition of 1 L of *warm* deionized water, the solid was filtered and washed with additional *warm* deionized water to remove sodium to below 0.02 wt %. After air-drying for several days under ambient conditions, the solid was made into a paste, and this paste was extruded through a Teflon die, dried, sieved to 0.85–2.0-mm particles, and calcined to 623 K by using a stepwise procedure.[3]

Cesium doping was effected by adding 2.5 g of the calcined pelletized catalyst to 25 mL of N_2-purged aqueous CsOOCH solution at 323 K. The solution was then evaporated to dryness under flowing N_2 (3–5 h). For all three M_2O_3-containing catalysts, a blank experiment was performed whereby the calcined catalyst was taken through the above doping procedure in water but with no cesium present. After doping, all catalysts were recalcined at 623 K for 3.0 h.

Catalyst Characterization. The catalysts were routinely examined in regard to surface area by gas adsorption using the BET method with argon (0.168 nm^2/Ar atom).[18,19] The samples were loaded under N_2 into Pyrex bulbs, evacuated overnight, and subsequently heated under dynamic vacuum (≈10^{-5} Torr) for 1 h at 383 K prior to argon gas adsorption measurements at 77 K.

X-ray powder diffraction patterns were obtained with a Philips diffractometer consisting of an XRG 3100 X-ray generator coupled with an APD 3600 control unit using Cu Kα radiation. Scans were taken with a 2θ step size of 0.01° and a counting time of 1 s unless otherwise stated. XRD was used for phase identification, for particle size measurement, and for monitoring lattice parameters. Air-sensitive samples, such as the reduced and tested catalysts, were loaded into an airtight sample holder[7] equipped with a Be window under dry nitrogen. XRD peaks of the Be window were used as a reference for calibration of the spectrometer. Air-insensitive samples were pressed into a standard Philips sample holder, and accurate d spacings were obtained by adding a reference silicon powder directly to the catalyst powder.

For analytical electron microscopy (AEM) analyses, a Philips EM-400T scanning transmission electron microscope was used for bright-field imaging (BFI), dark-field imaging (DFI), selected area diffraction (SAD), convergent-beam diffraction (CBD), and energy-dispersive spectroscopy (EDS) for X-ray elemental analysis in the scanning transmission mode (STEM). A 120-kV accelerating voltage was used in all analyses. A 10-nm spot size and a 100-s counting time were used for elemental identification and quantification by EDS. Integrated X-ray intensities were obtained by using a least-squares fitting routine. The intensities were quantified by using the thin-film approximation and

(6) Mehta, S.; Simmons, G. W.; Klier, K.; Herman, R. G. *J. Catal.* **1979**, *57*, 339.
(7) Bulko, J. B.; Herman, R. G.; Klier, K.; Simmons, G. W. *J. Phys. Chem.* **1979**, *83*, 3118.
(8) Nunan, J.; Klier, K.; Young, C.-W.; Himelfarb, P. B.; Herman, R. G. *J. Chem. Soc., Chem. Commun.* **1986**, 193.
(9) Klier, K.; Herman, R. G.; Young, C.-W.; *Prepr. Pap. Natl. Meet.—Am. Chem. Soc., Div. Fuel Chem.* **1984**, *29*(5), 273.
(10) Nunan, J. G.; Bogdan, C. E.; Klier, K.; Smith, K. J.; Young, C.-W.; Herman, R. G. *J. Catal.* **1989**, *116*, 195.
(11) Nunan, J. G.; Bogdan, C. E.; Herman, R. G.; Klier, K. *Catal. Lett.* **1989**, *2*, 49.
(12) (a) Reichle, W. T. U.S. Patent 4,458,026 (to Union Carbide Corp.), July 3, 1984. (b) Reichel, W. T. *J. Catal.* **1985**, *94*, 547.
(13) Bröcker, F. J.; Marosi, L.; Schröder, W.; Schwarzmann, M. German Patent 2,056,612 (to Badische Anilin- & Soda-Fabrik AG), May 31, 1972.
(14) Herman, R. G.; Simmons, G. W.; Klier, K. In *Proceedings of the 7th International Congrational Congress on Catalysis*; Seiyama, T., Tanabe, K., Eds.; Elsevier: Amsterdam, 1981; p 475. Although the identity of the hydrotalcite-like precursor was not explicitly mentioned, the diffraction pattern contained therein in Figure 1b unambiguously identified the hydrotalcite-like precursor of the Cu/ZnO/Al_2O_3 "micromonolith" catalysts.
(15) Gusi, S.; Trifiro, F.; Vaccari, A.; Del Piero, G. *J. Catal.* **1985**, *94*, 120.
(16) Nunan, J. G.; Herman, R. G.; Klier, K. *J. Catal.* **1989**, *116*, 222.
(17) Gherardi, P.; Ruggeri, O.; Trifiro, F.; Vaccari, A. In *Preparation of Catalysts III*; Poncelet, G., Grange, P., Jacobs, P. A., Ed.; Elsevier: Amsterdam, 1983, p 723.
(18) Anderson, J. R. *Structure of Metallic Catalysts*; Academic Press: New York, 1975.
(19) Herman, R. G.; Pendleton, P.; Bulko, J. B. In *Advances in Materials Characterization*; Rossington, D. R., Condrate, R. A., Snyder, R. L., Eds.; Plenum Press: New York, 1983, p 109.

Table I. Preparation Conditions and Purity of Different Hydrotalcite-like Precursors

HC-*n*	pH	sodium acetate present	temp, K	aging time, min	purity[a]
HC-3	6.5	no	353	10	0
HC-4	5.75–8.8	no	355	10	0.63
HC-5	5.8–8.8	no	333	10	0.84
HC-6	6.5	yes	333	10	0
HC-7	7.0	yes	333	10	0.80
HC-8	7.5	yes	333	10	0.53
HC-9	8.0	yes	333	10	0.86
HC-10	8.5	yes	333	10	0.94
HC-11	9.0	yes	333	10	0.98
HC-12	8.0	no	333	10	0.82
HC-13(a)	9.5	yes	333	5	1.0
HC-13(b)	9.5	yes	333	30	1.0
HC-14	9.0	yes	333	10	0.98
HC-15	9.0	yes	313	10	0.98
HC-16	9.0	yes	323	10	0.98
HC-17	9.5	yes	323	30	1.0
HC-18	9.5	yes	323	30	1.0
HC-20	9.65–10.94	no	323	30	1.0

[a] Hydrotalcite purity was taken as the XRD intensity ratio of peaks located at $2\theta = 11.8°$ for rhombohedral hydrotalcite and at 19.6° for the aurichalcite impurity phase by $I_{11.8°}/(I_{11.8°} + I_{19.6°})$.

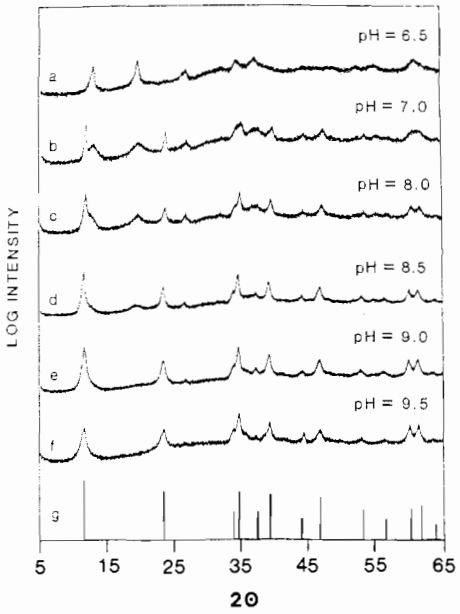

Figure 1. X-ray diffraction powder patterns showing the effect of pH on Cu/Zn/Al = 30/45/25 mol % hydrotalcite purity. Preparation conditions: $T = 60$ °C; aging time = 10 min; coprecipitated in the presence of sodium acetate at a pH of (a) 6.5 (HC-6), (b) 7.0 (HC-7), (c) 8.0 (HC-9), (d) 8.5 (HC-10), (e) 9.0 (HC-11), and (f) 9.5 (HC-13a) with 5-min aging time. Reference spectrum of hydrotalcite (g) is that from Busetto et al.[21]

applying the calculated Cliff–Lorimer factors[20] of $k_{Cu/Zn}$ and $k_{Al/Zn}$ equal to 0.956 and 0.719, respectively.

Results

A systematic study was carried out to specify the preparation procedure required to obtain a single-phase hydrotalcite-like precursor containig an intimate mixture of Cu + Zn + trivalent M. For the Cu/Zn/Al precursor as an example, the hydrotalcite-like samples prepared and the experimental conditions employed are tabulated in Table I, and the resultant XRD patterns of the precipitates are shown in Figure 1 as a function of pH. It

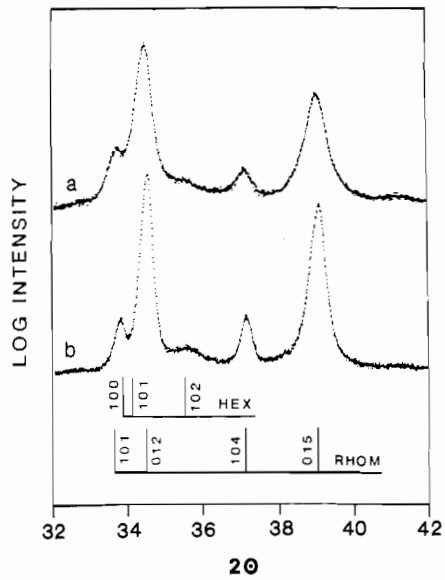

Figure 2. X-ray diffraction high-resolution scans in the 2θ range 32–42° (0.2° 2θ/min) for (a) the Cu/Zn/Al = 30/45/25 mol % precursor (HC-13) and (b) HC-13 after calcination and rehydration. Labeling is RHOM for the rhombohedral hydrotalcite structure and HEX for the hexagonal structure with corresponding *hkl* reflections.

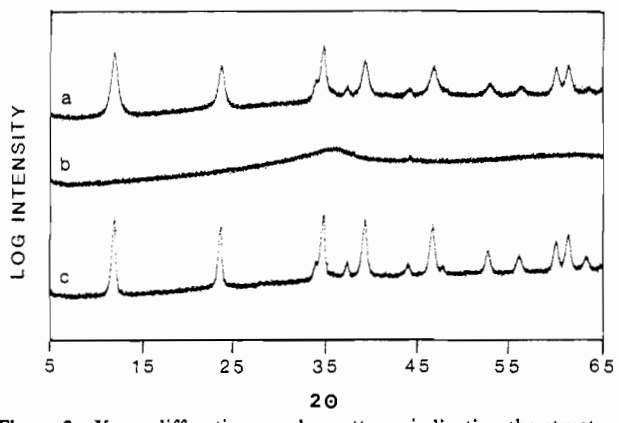

Figure 3. X-ray diffraction powder patterns indicating the structural changes that accompany the preparation steps of the Cu/Zn/Al = 30/45/25 mol % catalyst: (a) initial coprecipitated hydrotalcite-type precursor; (b) sample calcined at 623 K for 3 h; (c) re-formed hydrotalcite-type hydroxy carbonate after pelletization from an aqueous slurry. The broad peak centered at $2\theta = 35.6°$ in pattern b does not correspond to the rhombohedral hydrotalcite-type structure.

was found that the major impurity in the rhombohedral hydrotalcite-like samples was an aurichalcite hydroxy carbonate precursor, $(Cu,Zn)_5(OH)_6(CO_3)_2$.[5] The latter precursor was preferentially formed when the reaction medium was acidic. Upon increase of the pH, the percentage of the hydrotalcite-like precursor in the product increased until a pH ≥ 9.0 was achieved, where the precipitate consisted only of hydrotalcite.

The XRD peak located at $2\theta = 35.6°$ in Figure 1f does not correspond to the rhombohedral hydrotalcite structure. The XRD pattern obtained from a high-resolution scan (0.2° 2θ/min) is shown in Figure 2. The weak broad peak at 35.6° arises from a hexagonal form of hydrotalcite. The rhombohedral and hexagonal structures are very similar and only differ in the stacking sequence of adjacent brucite layers $[M^{II}_6M^{III}_2(OH)_{16}]^{2+}$ and the $[CO_3{\cdot}4H_2O]^{2-}$ interlayers.[22] A stacking sequence of –BC–CA–AB–BC– gives the rhombohedral structure, while the hexagonal structure has a sequence of –BC–CB–BC–. Thus, the c_0 unit cell dimension of the hexagonal structure is $\sim 0.67c_0$ for the rhombohedral configuration, while the a_0 lattice constant is very similar for the two structures. Most of the hydrotalcite-like samples

(20) Wood, J. E.; Williams, D. B.; Goldstein, J. I. *J. Microsc. (Oxford)* **1984**, *133*, 255.
(21) Busetto, C.; Del Piero, G.; Manara, G.; Trifiro, F.; Vaccari, A. *J. Catal.* **1984**, *85*, 260.
(22) Allmann, R. *Acta Crystallogr.* **1968**, *B24*, 972.

Table II. Lattice Parameters for the Original and Re-Formed Cu/Zn/Al = 30/45/25 Hydrotalcite-like Precursor with Silicon as an Internal Reference

precursor	a_0, Å	c_0, Å
original	3.0783 ± 0.0019	22.81 ● 0.25
re-formed in H_2O[a]	3.0779 ± 0.0012	23.01 ± 0.16
re-formed in Cs/H_2O[a]	3.0798 ± 0.0019	22.90 ± 0.11

[a] After calcination.

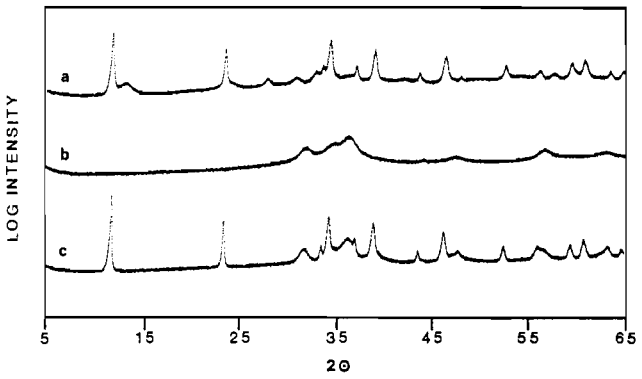

Figure 4. X-ray diffraction powder patterns indicating the structural changes that accompany the preparation steps of the Cu/Zn/Ga = 30/45/25 mol % catalyst: (a) initial hydrotalcite-type precursor; (b) sample calcined at 623 K for 3 h; (c) sample after cesium doping from an aqueous solution.

prepared contained small amounts of the hexagonal polymorph in addition to the predominant rhombohedral form.

During the preparation, temperature in the range 313–333 K and time of aging the precipitate within a 5–30-min range had little effect on the purity of the precursor formed. The use of sodium acetate in the reactant medium tended to give a purer hydrotalcite-like precursor than the use of pure distilled water.

XRD Analysis of the Calcined and Cs-Doped Cu/Zn/Al Catalysts. The XRD patterns of the HC-17 sample as prepared, the sample after calcination, and the sample after cesium doping are shown in Figure 3. It is evident that the rhombohedral hydroxy carbonate precursor was transformed into an amorphous phase by calcination to 623 K. The only feature in the resultant XRD pattern (Figure 3b) was a broad weak peak centered at $2\theta = 36°$, which is the general location of the strongest peaks of zincite ZnO and tenorite CuO. Doping the calcined catalyst with cesium resulted in regeneration of the rhombohedral hydrotalcite structure, as demonstrated by pattern c in Figure 3. A separate experiment in which the Cu/Zn/Al precursor was treated in the same sequence of steps as indicated in Figure 3, but with the absence of Cs in the rehydration solution, showed that the re-formation of the hydrotalcite precursor occurred even without the cesium. In each case, the XRD peak width in the pattern of the re-formed hydrotalcite-like samples, e.g. Figure 3c, was narrower than that for the original precursor, which indicates that the re-formed samples possessed enhanced crystallinity. Indeed, the peak width of the (015) diffraction line at 39° corresponds to a growth from 15.3 to 23.0 nm. At the same time, however, there was no change in the unit cell parameters, as shown in Table II. Recalcination of all of the hydrotalcite-like samples produced the featureless XRD pattern shown in Figure 3b.

XRD Analysis of the Calcined and Cs-Doped Cu/Zn/Ga Catalysts. The Cu/Zn/Ga precursor was prepared by using the experimental conditions described for Cu/Zn/Al preparation HC-17. The Cu/Zn/Ga = 30/45/25 system behaved similarly to the Cu/Zn/Al system. This is demonstrated by the effect of calcination and cesium doping on the XRD patterns shown in Figure 4. The XRD pattern of the precursor showed that a pure hydrotalcite-like phase was not formed. The impurity peaks correspond to aurichalcite. Calcination to 623 K caused decomposition of both hydroxy carbonates, and a weak broad set of peaks corresponding to ZnO appeared (Figure 4b). Rehydration of the calcined sample via the Cs-doping procedure resulted in the re-

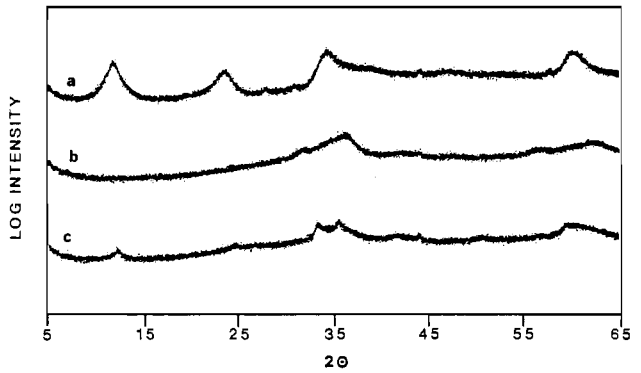

Figure 5. X-ray diffraction powder patterns indicating the structural changes that accompany the preparation steps of the Cu/Zn/Cr = 30/45/25 mol % catalyst: (a) initial hydrotalcite-like hydroxy carbonate precursor; (b) sample calcined at 623 K for 3 h; (c) sample after cesium doping from an aqueous solution.

Table III. Metal Ion Composition and Carbonate Content[a] of the Cu/Zn/Al and Cu/Zn/Cr Catalysts after Calcination at 623 K for 3.0 h[b]

catalyst	metal compn, atom %			
	Cu^{2+}	Zn^{2+}	M^{3+}	CO_3^{2-}/M^{3+}
$CuO/ZnO/Al_2O_3$	30.2	45.6	24.1	0.48
$CuO/ZnO/Cr_2O_3$	29.1	46.6	24.3	0.12

[a] Analyzed for metal ion composition and for C by Galbraith Laboratories, Inc., on samples that were sealed under a mild vacuum while still hot after calcination. [b] Metal salt solutions used for the precipitation of these catalysts had the composition of 0.30 M Cu^{2+}, 0.45 M Zn^{2+}, and 0.25 M M^{3+}. Note that a CO_3^{2-}/M^{3+} molar ratio of 0.5 would indicate no loss of carbonate during calcination.

formation of the hydrotalcite-like precursor but not the aurichalcite precursor. The XRD pattern shown in Figure 4c demonstrates that the re-formed hydrotalcite phase was more crystalline than the original precursor.

XRD Analysis of the Calcined and Cs-Doped Cu/Zn/Cr Catalysts. The XRD patterns obtained for the Cu/Zn/Cr = 30/45/25 system after precipitation, calcination, and cesium doping are shown in Figure 5. The Cu/Zn/Cr precursor was prepared by using the experimental conditions described for the Cu/Zn/Al HC-17 catalyst precursor (Table I). The initial precursor was very poorly crystalline (Figure 5a) and consisted of very small (≤5.6 nm) crystallites having the hydrotalcite-like structure. Calcination of the precursor at 623 K for 3 h led to a rather featureless XRD pattern with a single broad peak centered at $2\theta = 36°$, similar to that obtained with the Cu/Zn/Al sample (compare Figure 5b with Figure 3b). In contrast to the Cu/Zn/Al and Cu/Zn/Ga samples, doping the calcined Cu/Zn/Cr sample with CsOOCH did *not* result in significant re-formation of the hydrotalcite-like precursor (Figure 5c). Thus, for an identical metal ion mole fraction and similarly prepared and treated samples, the extent and onset of the re-formation phenomenon upon contacting the calcined materials with water was different for the Cu/Zn/Cr catalyst as compared with the Cu/Zn/Al and Cu/Zn/Ga hydroxy carbonate derived catalysts.

Chemical analysis of the calcined Cu/Zn/Al and Cu/Zn/Cr samples revealed a difference between these samples that could account for the observed difference in subsequent re-formation behavior. Analyses for metal ion and carbonate ion content are shown in Table III. It is evident that, after calcination, the carbonate content of the Cu/Zn/Al system was consistent with little or no loss of CO_2 during thermal decomposition ($CO_3^{2-}/Al^{3+} = 0.48$), whereas most of the carbonate was lost from the Cu/Zn/Cr catalyst precursor ($CO_3^{2-}/Cr^{3+} = 0.12$).

Re-Formation vs Al Content in Cu/Zn/Al Precursors. To separate the effects of chemical composition and crystallinity on the re-formation phenomenon, Cu/Zn/Al precursors were prepared with decreasing Al content but with a constant Zn/Cu ratio of ≈1.5. Figure 6 shows that altering the composition stepwise

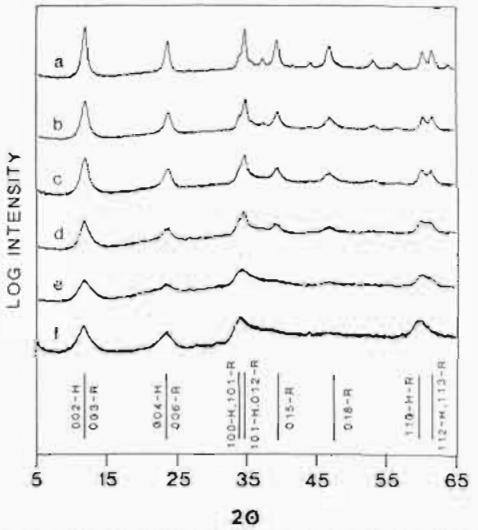

Figure 6. X-ray diffraction powder patterns of Cu/Zn/Al hydrotalcite-type precursors with varying Al contents compared with that produced by the Cu/Zn/Cr = 30/45/25 mol % precursor (f). Compositions of the Cu/Zn/Al samples are (a) 33/47/23, (b) 31/48/21, (c) 32/49/19, (d) 33/50/17, and (e) 34/51/15 mol %. The locations of major reflections (*hkl*) corresponding to the rhombohedral structure (R) and the hexagonal structure (H) of the hydroxy carbonate precursors are indicated.

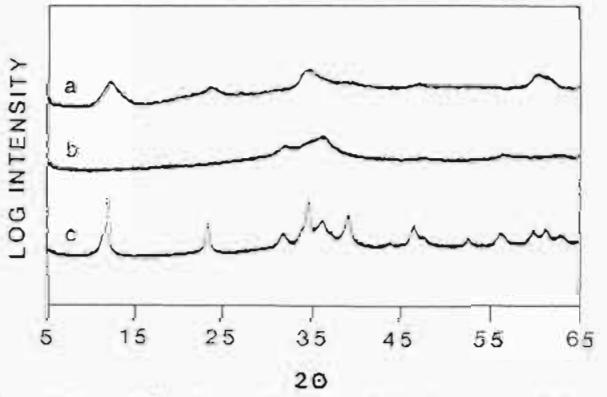

Figure 7. X-ray diffraction powder patterns indicating structural changes accompanying the preparation of a Cu/Zn/Al = 34/51/15 mol % catalyst: (a) initial hydroxy carbonate precursor; (b) sample calcined at 623 K for 3 h; (c) re-formed hydrotalcite-type hydroxy carbonate after equilibration in an aqueous solution to simulate cesium doping.

from Cu/Zn/Al = 30/47/23 to 34/51/15 mol % resulted in the systematic loss of crystallinity as detected by XRD. As indicated in the figure, the XRD pattern of the Cu/Zn/Al = 34/51/15 sample approximated that of the Cu/Zn/Cr = 30/45/25 hydrotalcite-like precursor. In no case was the presence of auricchalcite detected. With decreasing Al content, the relative peak intensities also changed. For example, comparison of the {100}-hexagonal and {101}-rhombohedral peak with the {101}-hexagonal and {012}-rhombohedral peak showed that the XRD intensity of the latter peak decreased much more than that of the former peak. Similarly, the peak due to the {112}-hexagonal and {113}-rhombohedral reflections decreased relative to the {110} peak. These observations indicate a greater loss of crystallinity or reduction in crystallite size in the ⟨001⟩ direction (c_0) relative to the ⟨100⟩ and ⟨110⟩ directions (a_0).

All of the Cu/Zn–Al precursors were calcined, and it was observed that a broad diffraction peak at $2\theta \approx 32°$ increased in intensity as the Al content of the samples decreased. The XRD pattern of the calcined Cu/Zn/Al = 34/51/15 sample is shown in Figure 7b. Upon treatment of this sample with water, re-formation of the hydrotalcite-type precursor was effected with a considerably enhanced degree of crystallinity (Figure 7c). Similar behavior was observed with all of the Cu/Zn/Al samples. Thus, re-formation of the calcined Cu/Zn/Al catalysts was independent of both the original overall chemical composition and the original degree of crystallinity of the samples under the experimental conditions employed.

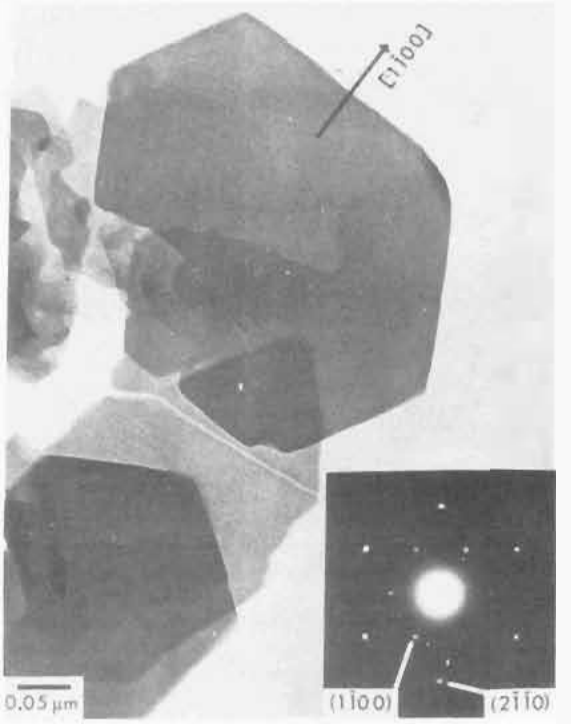

Figure 8. Transmission electron micrograph of the Cu/Zn/Al = 30/45/25 mol % hydroxy carbonate precursor and the corresponding selected area diffraction pattern, which is consistent with the (0001) plane being parallel to the platelet surface. The diffraction aperture (0.37 μm) was centered over the large labeled platelet.

Table IV. *d* Spacings (Å) and a_0 Lattice Parameters (Å) for the Hydrotalcite-like Cu/Zn/Al = 30/45/25 Precursors Determined from Selected Area Diffraction Patterns

sample	*d* spacing {1$\bar{1}$00}	*d* spacing {2$\bar{1}\bar{1}$0}	a_0
precursor			
XRD	2.67	1.54	3.08
Figure 8	2.68	1.54	3.09
EM exposure	2.58	1.49	2.98
calcined			
Figure 9	2.56	1.48	2.96
re-formed			
Figure 10	2.66	1.54	3.08

Electron Microscopic Analysis of the Cu/Zn/Al = 30/45/25 Catalyst. In contrast to XRD, EM can obtain imaging and diffraction data from individual particles. As shown in Figure 8, a platelet morphology was observed for the Cu/Zn/Al precursor, and it can be noted that the central particle has a size of ≈0.4 μm point-to-point. This is much larger than the apparent crystallite size of ≈15 nm determined by XRD. The SAD pattern shown in Figure 8 indicated that the (0001) plane of the hydrotalcite structure was parallel to the platelet surface. The a_0 lattice constant calculated from the SAD pattern was 3.09 Å, close to the 3.08 Å expected for the rhombohedral form of hydrotalcite (Table II). The {1$\bar{1}$00} diffraction spots indicated the presence of the hexagonal form of hydrotalcite, since these reflections are not generated by the rhombohedral structure. The {2$\bar{1}\bar{1}$0} reflections can be produced by both structure. Obtaining the SAD pattern after the particle was exposed to the electron beam for 5 min led to a set of smaller *d* spacings, as shown in Table IV. The smaller *d* spacings would be consistent with partial decomposition of the hydrotalcite-like platelets.

Calcination did not cause destruction of the large hexagonal-shaped platelets, but the surface of the particles appeared mottled. A platelet oriented perpendicular to the electron beam is shown

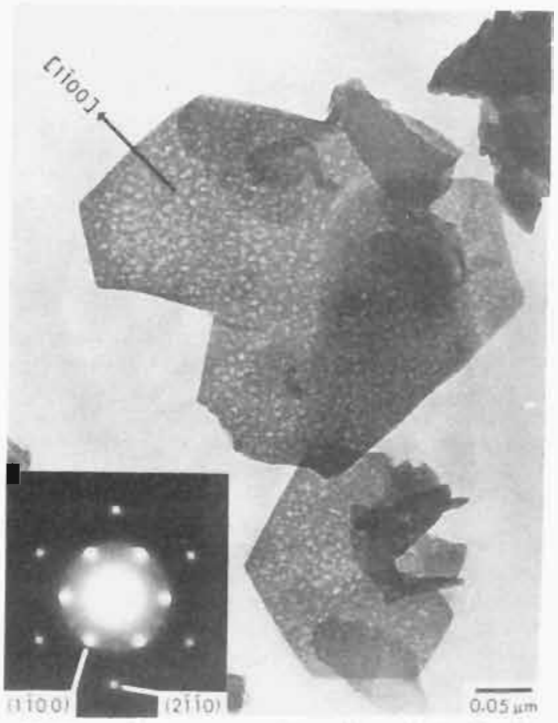

Figure 9. Transmission electron micrograph of the Cu/Zn/Al = 30/45/25 mol % sample after calcination at 623 K for 3 h and the corresponding selected area diffraction pattern, which was still consistent with a (0001) plane parallel to the platelet surface in a hexagonal lattice. The diffraction aperture (0.37 μm) was centered over the labeled platelet.

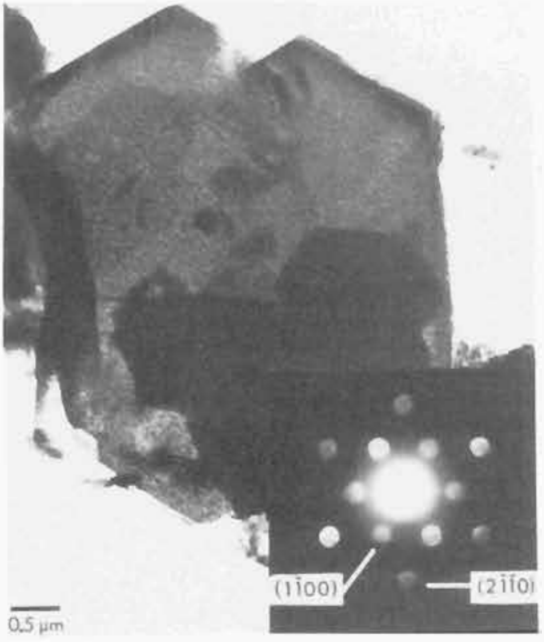

Figure 10. Transmission electron micrograph of the Cu/Zn/Al (30/45/25 mol %) re-formed hydrotalcite and the corresponding convergent beam (40 nm) diffraction pattern consistent with the (0001) plane parallel to the platelet surface.

in Figure 9, and the a_0 dimension and particular d spacings calculated from the SAD pattern are given in Table IV. It is seen that the dimensions observed with the calcined sample agreed very well with those determined with the sample that was subjected to prolonged exposure to the electron beam, indicating a contraction of the lattice induced by partial decomposition.

Electron microscopy of a re-formed Cu/Zn/Al sample produced the micrograph and convergent beam diffraction pattern shown in Figure 10. Particular lattice dimensions calculated from the diffraction pattern are given in Table IV, and it is evident that

Figure 11. Transmission electron micrograph of the Cu/Zn/Cr = 30/45/25 mol % hydrotalcite-type precursor and the corresponding selected area diffraction pattern.

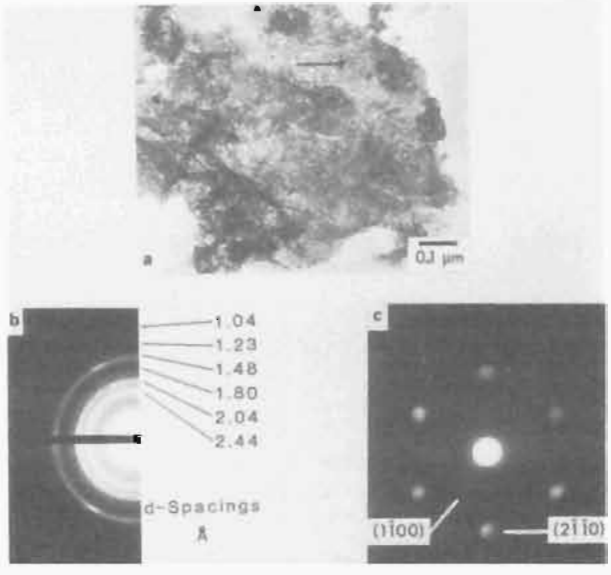

Figure 12. (a) Transmission electron micrograph of the Cu/Zn/Cr = 30/45/25 mol % calcined sample (623 K for 3 h) and (b) the selected area diffraction pattern, beside which the d spacings corresponding to the rings are given. The convergent beam (20 nm) diffraction pattern (c) from the arrowed location in (a) is consistent with a (0001) plane parallel to the platelet surface in a hexagonal lattice.

the hydrotalcite-like structure was re-formed by treatment with water.

Electron Microscopic Analysis of the Cu/Zn/Cr = 30/45/25 Catalyst. In contrast to the Cu/Zn/Al precursor, the Cu/Zn/Cr precursor did not consist of large well-defined hexagonal-shaped particles. Instead, the Cu/Zn/Cr precursor had a sheetlike morphology (Figure 11) that produced an SAD ring pattern, from which d spacings of 2.52 and 1.49 Å were calculated. These are similar to the values (Table IV) obtained for the Cu/Zn/Al sample subjected to a 5-min exposure to the electron beam and are characteristic of the hexagonal hydrotalcite structure. The sheetlike morphology of the Cu/Zn/Cr precursor might arise because of the flexibility of very thin hydrotalcite-like layers that results in significant folding.

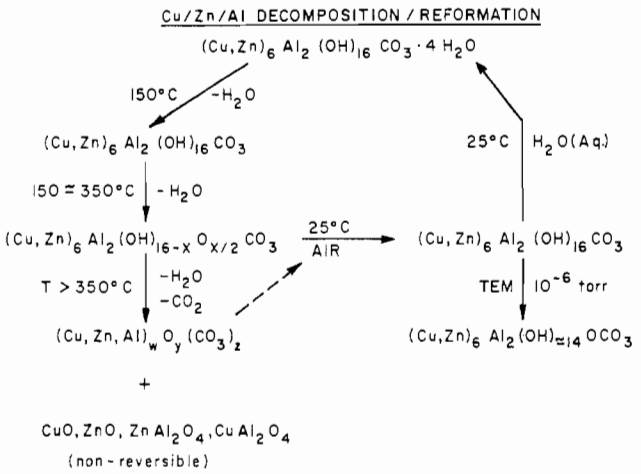

Figure 13. Proposed chemical and structural changes that accompany decomposition and re-formation of the $(Cu/Zn)_6Al_2(OH)_{16}CO_3{\cdot}4H_2O$ hydrotalcite-type precursor.

Calcination of the Cu/Zn/Cr precursor did not cause sintering of the sample (Figure 12). However, additional rings appeared in the electron diffraction pattern, and these seemed to be due to disordered oxides, e.g. ZnO, that have strong diffraction lines at 2.47 and 1.48 Å. However, other strong diffraction lines for ZnO at 1.62 and 1.91 Å were not clearly evident. The 1.48-Å ring was quite sharp and indicated preferred orientation relative to the other diffraction rings. The convergent beam diffraction pattern in Figure 12c exhibited an apparent 6-fold symmetry, and *d* spacings of 2.57 and 1.48 Å were calculated from the diffraction spots. These dimensions agree well with those corresponding to the $(1\bar{1}00)$ and $(2\bar{1}\bar{1}0)$ reflections of the hydrotalcite structure, and the pattern in Figure 12c most likely corresponds to a small portion of the hydroxy carbonate component that remained in the Cu/Zn/Cr precursor after calcination (see Table III) and that re-formed the hydrotalcite-like compound after rehydration (see Figure 5).

Discussion

The current study shows that the reconstitution of the mixed oxides of $CuO/ZnO/M_2O_3$ (M = Al, Cr, Ga) to their hydrotalcite-like precursors plays a critical role in the preparation of alkali-metal-doped methanol synthesis catalysts. The alkali-metal doping is carried out in aqueous suspensions of the $CuO/ZnO/M_2O_3$ mixed oxides that had been prepared by calcination of the hydroxy carbonates at 623 K. The reported loss of activity of the alumina-based catalysts and the observed little effect on the gallia-based catalysts upon doping with cesium[23] are elucidated by the presently observed re-formation of the hydrotalcite-type precursors, which results[16] in increased crystallinity (and lower surface area) and apparent burying of the cesium dopant. On the other hand, the Cs doping of the chromia-based catalysts results in successful catalysts that are not reconstituted into the hydroxy carbonate precursor during the doping procedure. Thus, cesium doping of the chromia-based catalyst results in a simple relationship between the doping levels and catalytic performance and gives the highest promotion effects achievable. This is reflected by the corresponding XRD spectra of the calcined catalysts before and after doping in Figures 3–5. Attributing the cause of the loss of activity to precursor re-formation upon cesium doping or water treatment is further substantiated by chemical analyses and by electron diffraction patterns obtained from individual particles during examination by transmission electron spectroscopy.

The cause of re-formation of the Al- and Ga-based catalysts as compared to the Cr-based catalysts is not dominated by differences in the catalyst crystallinity, as shown in Figures 6 and 7. It is related instead to the presence of Al or Ga (instead of Cr) in the ternary system with the resultant lack of complete decomposition (and retention of carbonate anions) during the calcination stage. Re-formation of the Cu/Zn/Al system may also be facilitated to some extent by the unique morphology/crystal structure of this system. During calcination, a topotactic decomposition of the precursor occurred, since the diffraction spots produced by the (0001) plane of the hydroxy carbonate precursor were aligned with the diffraction spots of the calcined sample. This is consistent with the ordered mechanism of thermal decomposition proposed for these layered hydroxy carbonates,[24-26] whereby water loss occurs with lattice contraction in the *c* direction and the metal–oxygen layers remain essentially intact up to temperatures of ≤723 K. The chemical composition up to this temperature is proposed to be $[(Cu,Zn)_6Al_2(OH)_{16-x}O_{x/2}]^{2+}CO_3^{2-}$, where water from the interlayer is completely removed at 473 K. Re-formation of samples heated at these lower temperatures (<623 K) begins by adsorption of water, which replenishes the OH^- species, followed by intercalation of H_2O in the interlayer $[CO_3{\cdot}4H_2O]^{2-}$. The above steps are summarized in Figure 13 for the Cu/Zn/Al system. For the case of the Cu/Zn/Cr system, a stabilizing factor might be the formation of a pre-spinel phase during the initial calcination at 623 K, which at higher temperatures would yield $CuCr_2O_4$ and $ZnCr_2O_4$. It has been demonstrated that a spinel-like phase was formed upon calcination of binary Zn–Cr coprecipitated precursors at 653 K.[27]

Acknowledgment. This research was supported in part by U.S. Department of Energy Contracts DE-FG22-83PC60786 and DE-AC22-84PC70021.

(23) Nunan, J. G.; Himelfarb, P. B.; Herman, R. G.; Bogdan, C. E.; Klier, K. To be submitted for publication.

(24) Taylor, H. F. W. *Mineral. Mag.* **1973**, *39*(304), 377 and references therein.
(25) Ross, G. J.; Kodama, H. *Am. Miner.* **1967**, *52*, 1036.
(26) Mumpton, F. A.; Jaffe, H. W.; Thompson, C. S. *Am. Miner.* **1965**, *50*, 1893.
(27) Del Piero, G.; Trifiro, F.; Vaccari, A. *J. Chem. Soc., Chem. Commun.* **1984**, 656.